ONSET OF SPACECRAFT CHARGING AND POTENTIAL JUMP IN GEOSYNCHRONOUS PLASMA

Jianguo Huang[(1,2)], Lixiang Jiang[(1,2)] , Song Wang[(1,3)] , Guoqing Liu[(1,2)]

[(1)]Beijing Institute of Space Environment Engineering, No.104, Youyi Street, Haidian District, Beijing, China, 100094. Email:huangjg2012@163.com

[(2)]Science and Technology on Reliability and Environmental Engineering Laboratory, No.104, Youyi Street, Haidian District, Beijing, China, 100094.

[(3)]Research Institute of Electrostatic and Electromagnetic Protection, Mechanical Engineering College, ShijiaZhuang, Beijing, 050003.

ABSTRACT

Geosynchronous spacecraft charging has been a focus of attention since a large number of satellites are operating in this region. The most severe geosynchronous charging environment is during substoms, in which the plasma environment is generally better described by double Maxwellian distribution. In such case, determination of onset of spacecraft charging becomes more complex since more parameters are involved. In this paper, the threshold condition for onset of charging in double Maxwellian plasma is developed theoretically in a more general sense, and the charging behavior at the threshold is investigated in detail. It is found that sudden jump to negative potential of thousands of volts or more can take place at the threshold in certain situation. The mechanism underlying the potential jump is clarified from the stability theory and illustrated by typical calculations. Moreover, a more general condition for potential jump is determined theoretically, and consequently another threshold condition for jump in positive direction is found. At both thresholds, the spacecraft potentials are semi-steady, but in opposite directions, with the possibility of a jump to a stable potential. The polarity of movement across the thresholds from different plasma will cause a spacecraft to experience irreversible charging histories which result in significant hysteresis. Generally, the jump to negative potential occurs with greater magnitude as compared to a potential jump in positive direction.

Keywords: spacecraft charging, geosynchronous plasma, threshold, potential jump

1. INTRODUCTION

Spacecraft charging can detrimentally affect electrical operations on space systems, especially for geosynchronous (GEO) spacecrafts, severe charging of thousands of negative voltages often occurs in disturbed plasma environment. The plasma density in geosynchronous environment varies from 0.1 cm^{-3} to more than 100cm^{-3}, and the energy varies from a few eV to tens of keV depending on local time and geomagnetic conditions [1]. The variable geosynchronous plasma is generated by more than two plasma sources like plasma sheet and the hot plasma population accelerated in magnetic storm, etc. Therefore the geosynchronous plasma is generally more precisely described by double Maxwellian distributions [2].

For a single Maxwellian plasma, Lai et al [3,4] and Laframboise et al [5] have proposed theoretically and also confirmed experimentally that the critical plasma parameter to determine severe spacecraft charging is plasma electron temperature, which is called the critical temperature, or threshold temperature, T*. Only above this critical temperature, severe negative charging can be triggered, while below it no severe charging can occur.

In double Maxwellian plasma, the onset of charging is more complex since more variables are involved. In addition, the triple-root-jump theory indicates that multiple roots exist for the current balance condition in some circumstances, and the potential may suddenly jump from an initial positive root (generally several volts) to a negative root of thousands of volts or more [6,7,8]. Although the principle and necessary conditions for the triple-root-jump are illustrated by diagrams in the literatures, more strict model or quantitative theory for the onset of potential jump is still needed for thoroughly understanding the phenomenon.

In this paper, a general theory to discribe the threshold condition for spacecraft charging and potential jump in double maxwellian plasma is developed, which is an extrapolation of our recent theoretical work [9]. In section 2, the theory of threshold for onset of spacecraft charging is first introduced. The behavior of spacecraft charging at threshold is studied for two typical cases. In section 3, the mechanism detailed process of potential jump is investigated. In section 4, a more general condition for potential jump based on stability of the potential is presented and discussed with respect to typical plasma conditions. In section 5, the two threshold conditions for potential jump, in both negative and positive directions, are constructed and demonstrated by calculation results. Finally, primary conclusions are drawn in section 6.

2. GENERAL THRESHOLD CONDITION FOR ONSET OF SPACECRAFT CHARGING

The space plasma environment varies in time. In the outer region of the geosynchronous orbit, energetic plasma clouds from the magnetotail may be injected around midnight during a substorm, and the energetic electrons tend to drift eastwards due to the curvature of the geomagnetic field. This is the socalled 'substorm injection' events, which may occur once in many days to a few times a day and last for hours each time. In quiet time, it is often a good approximation to describe the geosynchronous plasma with a Maxwellian energy distribution f (E). During substorms, it is often a better approximation to describe the disturbed plasma as a double Maxwellian [2], which is a sum of a low temperature, T_1, component and a high temperature T_2, component:

$$f(E) = f_1(E) + f_2(E) \quad (1)$$

$$f_1(E) = n_1\left(\frac{m}{2\pi k_B T_1}\right)^{3/2} \exp\left(-\frac{E}{k_B T_1}\right) \quad (2)$$

$$f_2(E) = n_2\left(\frac{m}{2\pi k_B T_2}\right)^{3/2} \exp\left(-\frac{E}{k_B T_2}\right) \quad (3)$$

where, n is the number density, m is the mass of electron or ion, and k_B is the Boltzmann constant. Here we have further surposed that electrons and ions both have the same distribution for each plasma component, i.e. $f_{ik} = f_{ek} = f_k$ (k=1, 2) with $n_{ik} = n_{ek} = n_k$ and $T_{ik} = T_{ek} = T_k$. For charging at threshold condition considered here, this approximation doesn't have significant influence to the result since the contribution by ions is far less than that of electrons. In addition, only shaded charging is considered since we are generally concerned with the more sever charging situations.

By convention, the first Maxwellian distribution f1 is the one with lower temperature, namely, $T_1 < T_2$. Suppose the spacecraft is initially uncharged, the current balance is between the incoming electron flux and the outgoing secondary and backscattered electron fluxes:

$$\frac{\int_0^\infty \int_0^{\pi/2} f(E)E(\delta+\eta)\sin\theta\cos\theta dEd\theta}{\int_0^\infty f(E)EdE\int_0^{\pi/2}\sin\theta\cos\theta d\theta} = 1 \quad (4)$$

Here, $\delta(E,\theta)$ and $\eta(E,\theta)$ are the angular dependent coefficients of secondary electron emission and backscattered electron emission, respectively, with θ the incidence angle of the primary electron. Substitute formula (1)-(3) into Eq.4, and after some complex algebra, the balance equation can be written in a simple form:

$$\frac{\alpha T_1^{1/2} < \delta+\eta >_1 + T_2^{1/2} < \delta+\eta >_2}{\alpha T_1^{1/2} + T_2^{1/2}} = 1 \quad (5)$$

In Eq.5, $\alpha = n_1/n_2$ denotes the density ratio of the two plasma components, and the following notation is used:

$$< \delta+\eta >_k = \frac{\int_0^\infty \int_0^{\pi/2} f_k(E)(\delta+\eta)\sin\theta\cos\theta E \cdot dEd\theta}{\int_0^\infty f_k(E)E \cdot dE \int_0^{\pi/2}\sin\theta\cos\theta d\theta} \quad (6)$$

This means averaging in terms of the kth energy distribution.

Then the left term of Eq.5 means the weighted average of the total averaged secondary and backscattered electron yields for each component, with weighting factor $\alpha(k_B T_1)^{1/2}$ for the T1 component and weighting factor $(k_B T_2)^{1/2}$ for T2 component, respectively. For convenience, a simple notation, $\overline{< \delta+\eta >_{1,2}}$, is used here. Then the threshold condition can be described as:

$$\overline{< \delta+\eta >_{1,2}} = 1 \quad (7)$$

With n_2=0 or ∞, the double Maxwellian distribution changes into single Maxwellian limit, and it can be obtained by Eq.5 that:

$$< \delta+\eta >= 1 \quad (8)$$

This is the threshold condition for onset of charging in single Maxwellian plasma, which is only a function of temperature [10].

Eq.7 gives more straightforward physical meanings: 1) The onset of spacecraft charging in a double Maxwellian space plasma is triggered at the condition that the weighted average of the total averaged secondary and backscattered electron yields equals to unity. The charging polarity over the threshold, $\overline{< \delta+\eta >_{1,2}} > 1$, will be discussed afterwards. 2) The charging threshold depends on the synergistic influence of T_1, T_2 and α (=n_1/n_2) as well, rather than depends only on T as in single Maxwellian plasma. It is the density ratio, rather than two separate densities, that is influential to the onset of spacecraft charging. 3) The threshold condition in single Maxwellian plasma is only a special case of Eq.7, therefore, the threshold described

by Eq.7 is a more general condition for onset of charging in geosynchronous environment.

To solve Eq.7 or 5, the angular dependent forms, $\delta(E,\theta)$ and $\eta(E,\theta)$, are needed, the formula given by [16] are used here:

$$\delta(E,\theta)=\delta(E,0)\exp\left[\beta_s(E)\cdot(1-\cos\theta)\right] \quad (9)$$

$$\eta(E,\theta)=\eta(E,0)\exp\left[\beta_b(E)\cdot(1-\cos\theta)\right] \quad (10)$$

Here, $\delta(E,0)$ and $\eta(E,0)$ are secondary electron and backscattered electron yield functions for normal incidence(θ=0) [6,12]:

$$\delta(E,0)=c\left[\exp(-E/a)-\exp(-E/b)\right] \quad (11)$$

$$\eta(E,0)=A-B\exp(-CE) \quad (12)$$

where, a=4.3E_{max}、b=0.367E_{max}、c=1.37δmax (δ_{max} is the maximum value for secondary emission function, and Emax is the primary electron energy associated with δ_{max}), and A, B, C are constants dependent on material properties.

β_s and β_b in Eq.9 and 10, are empirical factors. By fitting experimental data, Laframboise et al. [5] have obtained the forms of β_s and β_b:

$$\beta_s(E)=\exp(\xi) \quad (13)$$

$$\beta_b(E)=7.37Z^{-0.56875} \quad (14)$$

$$\xi=a\left(\ln\frac{E}{E_{max}}-b\right)-\left\{\left[a\left(\ln\frac{E}{E_{max}}-b\right)\right]^2+c\right\}^{1/2} \quad (15)$$

Here, a=0.2755, b=1.658, c=0.0228. The threshold condition is calculated with Cu-Be alloy, the material for the potential probe booms on the SCATHA satellite [13], as sample. The calculation is made for two typical cases: 1) $T_A<T_1<T^*<T_2$ and 2) $T_1<T_A<T_2<T^*$, where T^* and T_A are the critical temperature and anticritical temperature [14], respectively, at which the total averaged coefficients of secondary and backscattered electron emission, $<\delta+\eta>$, equals to unity. The threshold condition for case 1 and case 2 are demonstrated in fig.1 and fig.2, respectively. The material parameters are taken as follows: E_{max}=0.3keV, δ_{max}=4.2, A=0.3136, B=0.0692 and C=0.0016. In the two figures both thresholds for normal incidence and isotropic plasma are presented for comparison, and also the plots of $<\delta+\eta>$ for normal ($<\delta+\eta>_{norm}$) and isotropic incidence ($<\delta+\eta>_{iso}$) are given for convenient understanding, with T_A (9eV for normal and 7.2eV for isotropic incidence) and T^* (2.4keV for normal and 3.5keV for isotropic incidence) designated by vertical dotted lines.

The results indicate that the threshold condition for case 1 and case 2 show different features. For case 1 (see fig.1, T_2=28keV), the threshold condition is limited between $T_1=T_A$ and $T_1=T^*$, positive charging occurs above the threshold (dark gray region) and negative charging occurs below the threshold. Since the net electron current by the T_2 ($>T^*$) component is incoming, only when the T_1 falls between T_A and T^* it can provide outgoing electron current and the current balance is satisfied. While for case 2 (see fig.2, T_2=0.5keV) the threshold displays as two branches, located in $T_1<T_A$ and $T_1>T^*$, respectively. The result is due to the fact that the net electron current by T_2 component ($T_A<T_2<T^*$) is outgoing, as a result only when the T_1 component ranges in $T_1<T_A$ or $T_1>T^*$ the resultant electron flux is incoming and a competition can occur. For case 2, positive charging (dark gray) occurs below the threshold and negative charging above it, in contrast to the situation in case 1.

Fig.1 and fig.2 also show that the threshold condition for isotropic plasma is shifted to lower T_A and higher T^* compared with normal incidence situation. It's interesting that the critical temperature T^* and anticritical temperature T_A defined in single Maxwellian plasma both play important roles in the double Maxwellian plasma threshold condition. In the calculations and discussions afterwards, only the normal incidence situation is considered for simplicity, and the conclusion drawn are also applicable to the isotropic situation.

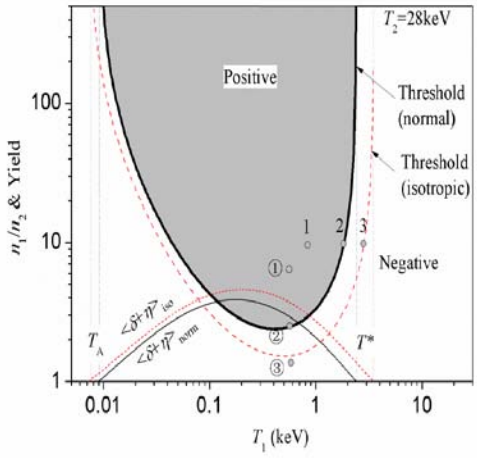

Figure.1, The threshold condition and averaged coefficients of secondary and backscattered electron emission for Cu-Be alloy (case 1: T_2=28 keV).

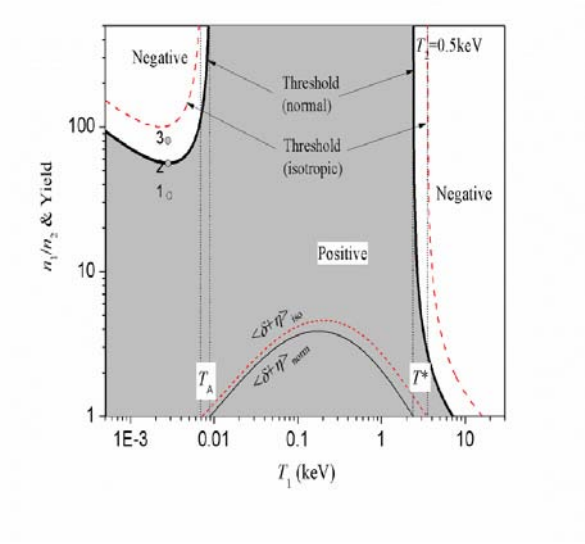

Figure.2, The threshold condition and averaged coefficients of secondary and backscattered electron emission for Cu-Be alloy (case 2: T_2=0.5 keV).

3. POTENTIAL JUMP AT THRESHOLD CONDITION

3.1. Charging Equations

The evolvement of surface potential can be described by:

$$J_{net}(\phi)=\frac{C_s}{A}\frac{d\phi}{dt} \tag{16}$$

Here, J_{net} is the net charging current, it is a function of the surface potential ϕ. C_s/A is capacitance per unit area, and C_s/A ~$\varepsilon_0 R$ for metal surface (ε_0 is the dielectric constant for vacuum and R the radius of the surface curvature). By convention, the current by the incident ions is defined as positive. Then the charging current in eclipse can be described as [6,11]:

$$J_{net}(\phi)=\sum_{k=1}^{2}\left\{J_{i0k}\left(1+Q\right)-J_{e0k}\exp\left(-Q\right)\left(1-<\delta+\eta>_k\right)\right\}$$

for $\phi<0$ (17a)

$$J_{net}(\phi)=\sum_{k=1}^{2}\left\{J_{i0k}\exp\left(-Q\right)-J_{e0k}\left(1-<\eta>_k\right)\left(1+Q\right)+J_{e0k}<\delta>_k\exp\left(-\frac{e\phi}{k_BT_s}\right)\left(1+\frac{e\phi}{k_BT_s}\right)\right\}$$

for $\phi>0$ (17b)

Here, $Q=e|\phi|/k_BT_k$ and e is the electron charge, J_{e0k} and J_{i0k} are the initial incident electron and ion current density at ϕ=0 for the kth component, and T_s is the temperature for secondary electrons, generally at 2~3 eV. The potential at equilibrium can be obtained by Eq.17 with $J_{net}(\phi)$=0.

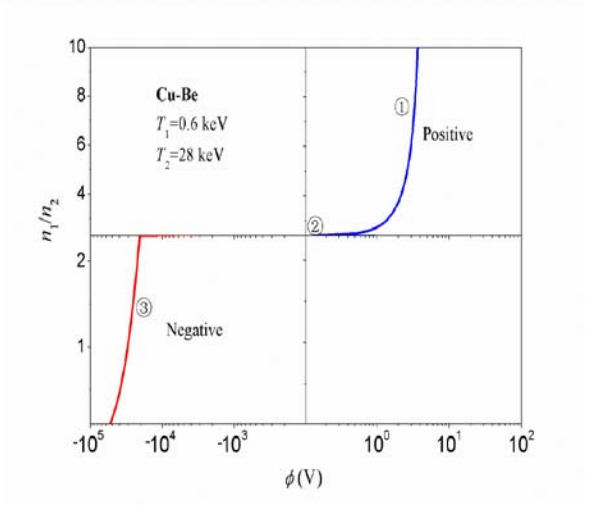

Figure.3, Potential variation with the density ratio of the two plasma components for case 1 ($T_A<T_1<T^*<T_2$, T_1=0.6KeV, T_2=28KeV)

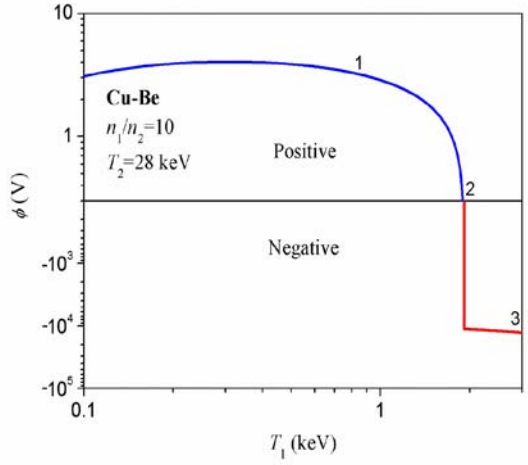

Figure.4, Potential variation with temperature T_1 for case 1 ($T_A<T_1<T^*<T_2$, n_1/n_2=10, T_2=28KeV)

3.2. Case 1: $T_A<T_1<T^*<T_2$

The case $T_A<T_1<T^*<T_2$ is the typical situation in GEO plasma environment during substorms with injection of energetic plasma cloud (T_2) of tens of keV. The background plasma frequently falls in $T_A<T_1<T^*$. For Cu-Be alloy sample used here, T_A=9eV and T^*=2.4keV. At the threshold, both variations of temperature and the density ratio can trigger spacecraft charging. The charging induced by the density ratio variation at fixed

temperature is shown in fig.3 (T_1=0.6keV, T_2=28keV), it's clear that the potential jumps suddenly to a negative value (-20.82kV) at the threshold as the density ratio decreases along ①→②→③ (see fig.1). Similarly, potential jump is also triggered by temperature variation at the threshold, as illustrated in fig.4 (T_2=28keV, n_1/n_2=10). The potential jump at the threshold will be discussed afterwards.

3.3. Case 2: $T_1<T_A<T_2<T^*$

In some circumstances, there exists a cloud of low energy electrons (typically with $T<T_A$) around the spacecraft, for example, the secondary electrons trapped around the spacecraft due to differential charging, the artificial plasma by electric engine plume, etc. The mechanism of low energy electron cloud formation is outside the scope of this paper. In the case $T_1<T_A<T_2<T^*$, the variation of potential as the density ratio increases with fixed T_1 is shown in fig.5 (T_1=3eV , T_2=0.5keV). As the first plasma changes along 1→2→3 (see fig.2), the potential transits from positive to negative continuously around the threshold, which is remarkably different from case 1. The potential transition at the threshold induced by temperature variation is continuous, too, which is not presented here.

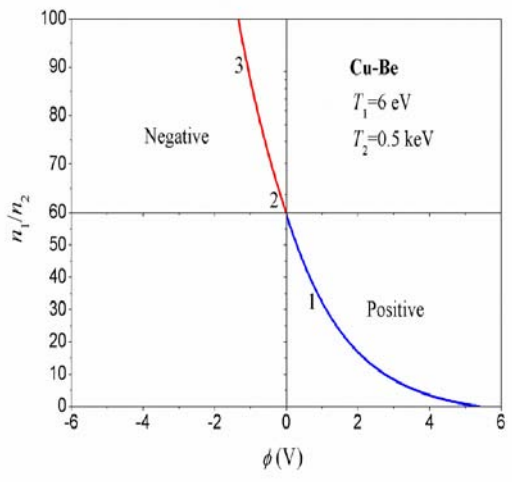

Figure.5, Potential transition with decreasing of the density ratio for case 2 ($T_1<T_A<T_2<T^*$, T_1=6eV, T_2=0.5keV).

3.4. Mechanism For Potential Jump

A steady potential at which the spacecraft is charged must be a solution to the current balance equation $I_{net}(\phi)=0$. Take ϕ_0 as the equilibrium potential and assume a small initial perturbation, $\delta\phi_0$, such that $\phi=\phi_0+\delta\phi_0$, where $\delta\phi_0 << \phi_0$, then it can be obtained from Eq.16 that $\delta\phi$ develops as follows [11,15]:

$$\delta\phi=\delta\phi_0\exp\left[C_s t/\left(dJ_{net}/d\phi\right)_{\phi=\phi_0}\right]. \quad (18)$$

For a steady potential, the perturbation must attenuate automatically, i.e. $\delta\phi\to 0$, or the necessary condition for a steady potential is:

$$\left.\frac{dJ_{net}}{d\phi}\right|_{\phi=\phi_0}<0 \quad (19)$$

Otherwise, if any of the following two situations occur:

$$\left.\frac{dJ_{net}}{d\phi}\right|_{\phi\to\phi_0^-}>0 \text{ and } \left.\frac{dJ_{net}}{d\phi}\right|_{\phi\to\phi_0^+}<0 \quad (20a)$$

or

$$\left.\frac{dJ_{net}}{d\phi}\right|_{\phi\to\phi_0^+}>0, \text{ and } \left.\frac{dJ_{net}}{d\phi}\right|_{\phi\to\phi_0^-}<0 \quad (20b)$$

The potential can't stay stable and sudden jump will occur. In the former situation, described by inequality (20a), the potential ϕ_0 is unstable for negative perturbation and will jump to a stable solution ϕ_1 with more negative value, as illustrated by fig.6 (a). Such situation is like a ball on top of a downward slope on the left (see fig.6(a), lower plot), even a minimal perturbation leftwards will lead the ball to slip downwards to its left until reaching a stable position. While for the latter situation depicted by inequality (20b), the potential is unstable for positive perturbation and jump to a more positive steady potential will happen (see fig.6(b)). In both of the situations, the initial solution ϕ_0 is at a 'semi-steady' state, only when the potential satisfying Eq.19 can appear as a equilibrium potential, like a ball staying at the bottom of a concave (see fig.6(c)), any perturbation of displacement will attenuate automatically and the ball can stay at the bottom steadily, such a state is a 'fully-steady' state.

To clarify the mechanism and detailed process of potential jump for case 1, a small perturbation $|\delta\phi_0|$ of 2V, both negative and positive, is exerted to the initial potential at the threshold (ϕ_0=0), the resultant potential and current evolvements are shown in fig.7. For negative perturbation with $\delta\phi_0$=-2V (see fig.7 (a)), the exponential decrease of the outgoing electron current J_{e1} dominates the change of J_{net} in the beginning since $T_1>>T_2$ (see Eq.17(a)), resulting in a rapid decrease of

J_{net} and subsequent positive $dJ_{net}/d\phi$. As a result the perturbation increases according to Eq.18. As the perturbation surpasses a certain value (here about -2kV) J_{net} is pulled back again by the increasing J_i and decreasing incoming J_{e2}, until J_{net} returns to zero again and a new steady solution is reached. While for the positive perturbation with $\delta\phi_0$=2V (see fig.7 (b)), positive $dJ_{net}/d\phi$ exists forever, because the outgoing secondary electron current of J_{e1} decreases at moderate positive potential, and more electrons are attracted and ions are repelled at larger positive potentials. As a result, the positive perturbation $\delta\phi_0$ will attenuate according to Eq.18 and eventually regress to the initial potential (ϕ_0 =0). In summary, the threshold condition for case 1 is a semi-steady state, which is unstable for a negative perturbation, the potential jump in negative direction will take place.

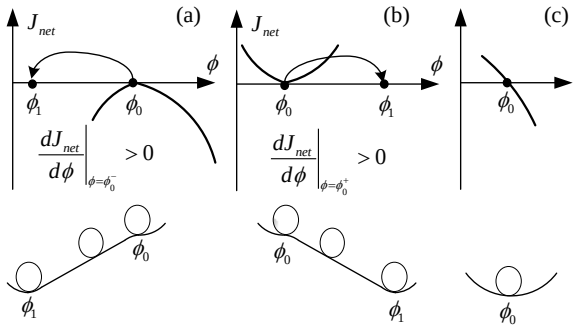

Figure.6, Diagram of stability of a solution and the situation for potential jump. (a) The solution is unstable on the negative side and tends to jump negatively. (b) The solution is unstable on the positive side and tends to jump positively. (c) The solution is stable.

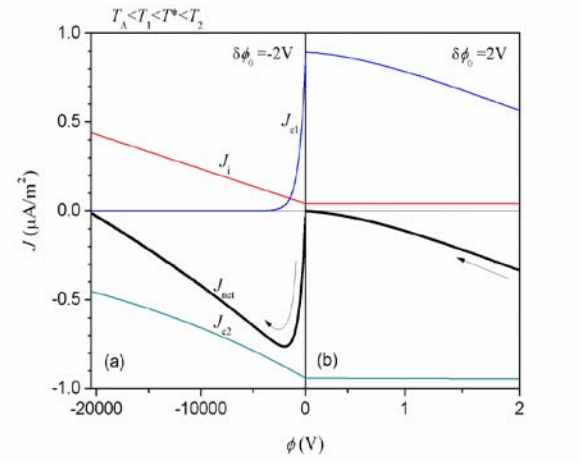

Figure.7, The evolvement of the solution at the threshold condition for case 1 with (a) a small negative perturbation and (b) a positive perturbation to the initial potential, the magnitude of perturbation is 2V (T_1=0.6keV, T_2=28keV, n_1/n_2=2.4).

For the threshold condition for case 2, the potential and current evolvements with a small perturbation are shown in fig.8. For both negative and positive perturbations, the potential always comes back to its initial state (ϕ_0 =0), since $dJ_{net}/d\phi$ is negative on both sides. The threshold condition for case 2 is fully-steady, therefore, potential jump can't occur at the threshold.

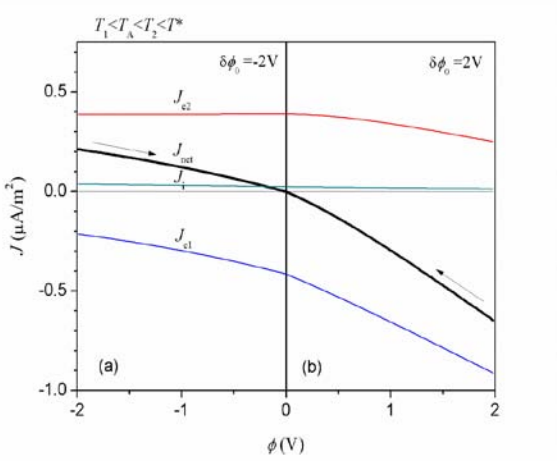

Figure.8, The evolvement of the solution at the threshold condition for case 2 with a small (a) negative perturbation and (b) positive perturbation to the initial potential (T_1=3eV, T_2=0.5keV, n_1/n_2=60)

4. GENERAL CONDITION FOR POTENTIAL JUMP

4.1. Necessary Condition For Potential Jump

Suppose the spacecraft is initially charged at ϕ_0, which is a root of the balance equation, $J_{net}(\phi_0)=0$. According to the theory in section 3.4, for potential jump to take place at ϕ_0, the following condition has to be satisfied:

$$dJ_{net}/d\phi\big|_{\phi\to\phi_0^-}\cdot dJ_{net}/d\phi\big|_{\phi\to\phi_0^+}<0 \qquad (21a)$$

Inequality (21a) is equivalent to inequality (20a) and (20b), if $dJ_{net}/d\phi$ is a continuous function at ϕ_0, the above condition can also be described as:

$$\begin{cases} dJ_{net}/d\phi\big|_{\phi\to\phi_0}=0 \\ d^2J_{net}/d\phi^2\big|_{\phi\to\phi_0}\neq 0 \end{cases} \qquad (21b)$$

The physical meaning of condition (21a) or (21b) is that, when the differential $dJ_{net}/d\phi$ changes its polarity at

opposite sides of ϕ_0, the potential must be unstable at one side and a minimal perturbation to the potential can trigger it to jump to the unstable side with positive $dJ_{net}/d\phi$.
On the basis of above arguments, we will examine the potential jump condition in a more general sense.

4.2. Discussion For $\phi_0 > 0$

For the spacecraft initially charged positively (ϕ_0 >0), we can easily obtain from Eq.17b:

$$dJ_{net}/d\phi\big|_{\phi\to\phi_0} < 0, \text{ for } \phi_0 > 0 \qquad (22)$$

As discussed earlier, it is a fully-steady solution. Therefore, we conclude that it's impossible for potential jump to take place if the spacecraft is initially charged positively.

4.3. Discussion for $\phi_0 = 0$ (threshold condition)

If the spacecraft is initially uncharged ($\phi_0 = 0$), which is the case for the threshold condition, the potential transition has thoroughly discussed above. For case 1: $T_A<T_1<T^*<T_2$, the requirement for unsteady solution, inequality (20a), is always satisfied, so potential jump in negative direction always takes place at the threshold (see fig.3, 4 and 7). While for case 2: $T_1<T_A<T_2<T^*$, it has been verified that the necessary condition for a steady solution Eq.19 is always satisfied [9], therefore we conclude that potential jump is impossible to occur in case 2, and the potential transits smoothly as the threshold is crossed (see fig.5 and 8).

4.4. Discussion For $\phi_0 < 0$

Now we consider the situation that the spacecraft is initially charged at negative potential (ϕ_0 <0). ϕ_0 is a negative root of the current balance equation, then from Eq.(17a), there is:

$$\sum_{k=1}^{2}\left\{J_{i0k}\left(1-\frac{e\phi_0}{k_BT_k}\right)-J_{e0k}\exp\left(\frac{e\phi_0}{k_BT_k}\right)\left(1-<\delta+\eta>_k\right)\right\}=0 \quad (23)$$

If potential jump occurs at ϕ_0, according to Eq.(21b) we have:

$$\sum_{k=1}^{2}\left\{\frac{1}{k_BT_k}J_{i0k}+\frac{1}{k_BT_k}J_{e0k}\exp\left(\frac{e\phi_0}{k_BT_k}\right)\left(1-<\delta+\eta>_k\right)\right\}=0 \quad (24)$$

Eliminating n_1/n_2 form Eq.23 and 24, after some algebra we obtain the following equation:

$$\sqrt{m_e/m_i}\left[k(T_1+T_2)-e\phi_0\right]\left[\frac{\exp(e\phi_0/kT_2)}{<\delta+\eta>_1-1}+\frac{\exp(e\phi_0/kT_1)}{1-<\delta+\eta>_2}\right] \qquad (25)$$
$$=k(T_2-T_1)\left[\exp\left(\frac{T_1+T_2}{kT_1T_2}e\phi_0\right)+\frac{m_e/m_i}{(<\delta+\eta>_1-1)(1-<\delta+\eta>_2)}\right]$$

It is the necessary condition for an unsteady solution ϕ_0, at which potential jump will occur. Now let us examine the feature of Eq.25 for case 1 and case 2, respectively.
For case 2: $T_1<T_A<T_2<T^*$, $<\delta+\eta>_1<1$ and $<\delta+\eta>_2>1$, the terms on the left and right sides of Eq.25 have opposite polarities, therefore there is no solution to the equation, such that potential jump can't occur in case 2. While for case 1: $T_A<T_1<T^*<T_2$, we have $<\delta+\eta>_1>1$ and $<\delta+\eta>_2<1$, the terms on both sides of Eq.25 are of the same polarity, thus it is possible to find solution to the equation.

5. THRESHOLD CONDITIONS FOR POTENTIAL JUMP

Now we try to build the threshold conditions for the two types of potential jump in case 2, the jump to positive potential and the jump to negative potential, respectively. Solve Eq.25 numerically and substitute the solution ϕ_0 (<0) into Eq.23, one obtain the threshold condition for the potential jump from initial negative potential to a final positive value:

$$\alpha=\sqrt{\frac{T_2}{T_1}}\frac{\exp(e\phi_0/kT_2)(1-<\delta+\eta>_2)-\sqrt{m_e/m_i}(1-e\phi_0/kT_2)}{\exp(e\phi_0/kT_1)(<\delta+\eta>_1-1)+\sqrt{m_e/m_i}(1-e\phi_0/kT_1)}, \quad (26)$$

The threshold for the potential jump is shown in fig.9, designated by 'Threshold_'. Another jump occurs at the threshold condition for onset of charging described by Eq.7, as discussed in section 4.3, which is also drawn in the figure for comparison, since it's also a threshold for potential jump, it's designated by 'Threshold$_0$' for distinguishing. Here the subscripts, $_0$ and $_-$, suggest the initial charging status for the jump.
The flux-voltage plots for some points in the parametric domain (point 1~5 in fig.9) are illustrated in fig.10, in which the curves for the positive potential are drawn diagrammatically. It is clearly demonstrated that two potential jumps altogether come up: at point 2 which is located at threshold$_0$, the potential jumps from initial zero to a final negative value, while at point 4 located at threshold_, the potential jumps from initial negative value to a final positive value. In addition, the jump at threshold_ appears with more significant magnitude compared with that at threshold$_0$, as illustrated in fig.10.
As shown by fig.9, the threshold condition threshold_ is located within the region enclosed by the threshold

threshold$_0$, or the threshold for charging onset, and the two thresholds coalesce at the lower limit T_A and upper limit T^*, respectively. The triple-root domain appears as meniscus shape in the assumption of $n_{ik}=n_{ek}$. Fig.9 and 10 both show that the region between the two thresholds is the triple-root parametric domain, e.g. the J_{net}-ϕ curve for point 3 has three roots (see fig.10, the curve for point 3).

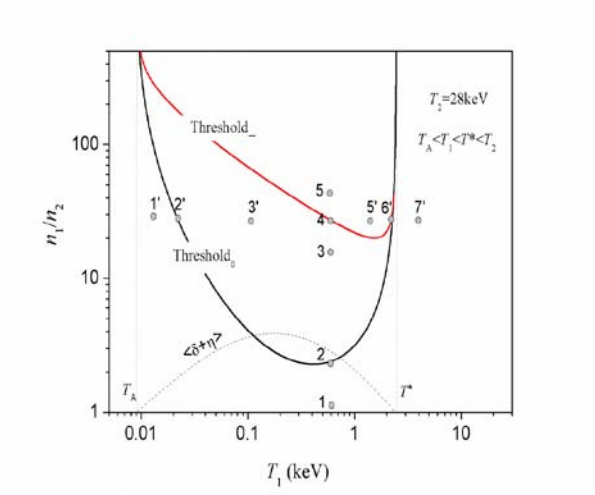

Figure.9, Threshold conditions for *potential jump with zero and negative initial potentials, respectively, for case* 1.

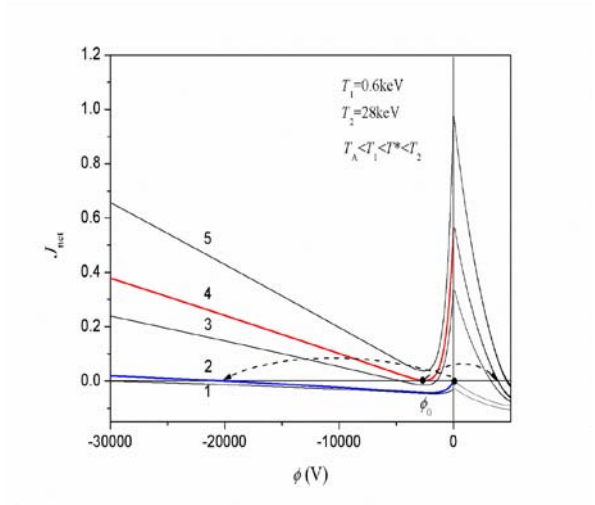

Figure.10, Net charging current as a function of potential for point 1~5 in fig.9.

The charging histories by passing through different parametric domains and returning in opposite direction are presented in fig.11 and fig.12, which show clear hysteresis, namely, potential jump depends on the initial charging state and charging history, which is consistent with the conclusion in reference [7]. The hysteresis is due to the fact that the jump to negative potential and the jump to positive potential take place at different thresholds.

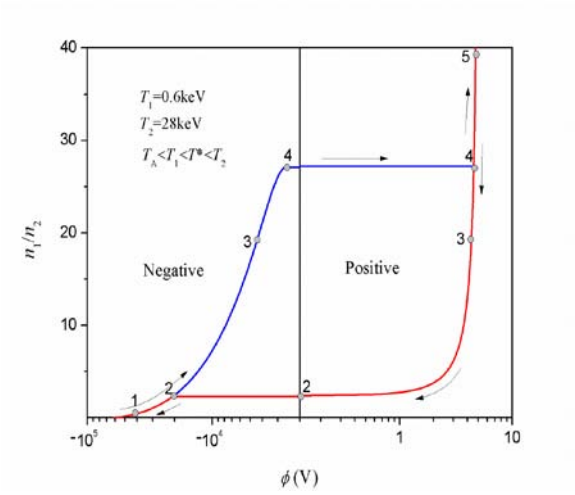

Figure.11, History of potential evolvement as the density ratio n_1/n_2 increases passing through points 1→5 in fig.9 and subsequently decreases (on the return trip), the initial potential being negative.

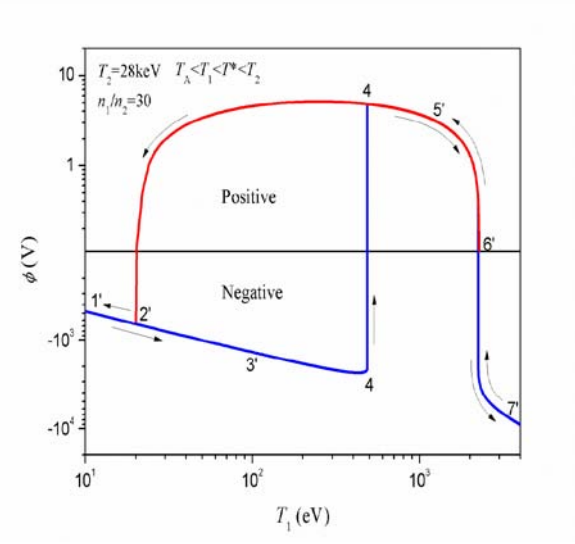

Figure.12, History of potential evolvement as T_1 increases passing through points 1'→7' and subsequently decreases (on the return trip).

6. CONCLUSION

The threshold condition for onset of charging in double Maxwellian plasma is theoretically studied. With isotropic plasma taken into account, the threshold condition has the same formation with normal incidence. The threshold condition indicates that when the weighted average of the total secondary and backscattered electron yields equals to unity surface charging can be triggered. The onset of charging is

determined by the relative density ratio and the temperatures. For isotropic plasma, the threshold is shifted towards lower T_A and higher T^*.

The behavior of charging at the threshold is investigated for two typical cases in GEO plasma environment. In case 1, $T_A<T_1<T^*<T_2$, negative charging takes place in the manner of sudden potential jump from initial zero potential. While in case 2, $T_1<T_A<T_2<T^*$, the potential develops continuously around the threshold. The mechanism for potential jump can be interpreted from the view point of stability of the equilibrium potential. At the threshold, the potential (zero) is in a semi-steady state, which is unstable for a negative perturbation and will jump to a stable negative potential.

More general threshold condition for potential jump is investigated, it's found that there are two thresholds for potential jump altogether, both of which occur in case 1. One is just the threshold for onset of charging, which is unsteady in the negative direction and jump to negative potential will happen. Another threshold for jump is unsteady in the positive direction and jump from initial negative to positive potential will take place. The latter threshold condition is located within the domain enclosed by the first threshold, and the two thresholds coalesce at the lower limit T_A and upper limit T^*, respectively. The parameter region between the two thresholds is the triple-root domain, in which both positive and negative charging is possible. The triple-root domain appears as meniscus shape in the assumption of $n_{ik}=n_{ek}$.

Due to the fact that the potential jumps in positive and negative directions occur at different threshold conditions, as crossing the thresholds and returning in the same path, the charging processes are irreversible and hysteresis can be observed. Generally, the potential jump in the negative direction happens in a more significant magnitude than the jump in positive direction.

7. REFERENCES

1. Gussenhoven M. S. (1982), Geosynchronous Environment for Severe Spacecraft Charging, J. Spacecraft and Rockets, 20(1), 26-34.
2. Garrett and DeForest (1979), An analytical simulation of the geosynchronous plasma environment, Planetary Space Science, 27, 1101-09.
3. Lai, S. T., Gussenhoven, M. S. and Cohen, H. A. (1982), Energy range of ambient electrons responsible for spacecraft charging, Eos Trans. AGU, 63(18), 421.
4. Lai, S. T., Gussenhoven, M. S. and Cohen, H. A. (1983), The concepts of critical temperature and energy cut-off ambient electrons in high voltage charging of spacecraft, in Proceedings of the 17th ESLAB symposium, edited by D. Guyenne and J. H. A. Pedersen, 169-175, Eur. Space Agency, Noordwijk, Netherlands.
5. Laframboise, J. G., Godard, R. and Kamitsuma, M. (1982), Multiple floating potentials, threshold temperature effects, and barrier effects in high voltage charging of exposed surfaces on spacecraft, paper presented at International Symposium on Spacecraft Materials in Space Environment, Eur. Space Agency, Toulouse, France.
6. Prokopenko, S. M. L. and Lamframboise, J. G. (1980), High-voltage differential charging of geostationary spacecraft, Journal of Geophysical Research, 85(48), 4125-31, doi: 10.1029/JA085iA08p04l25.
7. Lai, S. T. (1991a), Spacecraft charging thresholds in single and double Maxwellian space environment, IEEE transactions on Nuclear Science, 38(6), 1629.
8. Lai, S. T. (1991b), Theory and observation of triple-root jump in spacecraft charging, Journal of Geophysical Research, 96 (A11), 19269-19281.
9. Huang J G, Liu G Q and Jiang L X (2015), J. Geophys Res. Space Physics. 120, 6301-6308.
10. Lai S. T. and Devin J. Della-Rose (2001), Spacecraft charging at geosynchronous altitudes: new evidence of existence of critical temperature, Journal of Spacecraft and Rockets, 38 (6).
11. Hastings D. E. and Garrett H. (1996), Spacecraft-environment interaction, Cambridge University Press, 156-157.
12. Sanders, N. I., and Inouye, G. T. (1978), Secondary emission effects on spacecraft charging: Energy distribution, Spacecraft Charging Technology, edited by R. C. Finke and C. P. Pike, 747-755, U. S. Air Force Geophys. Lab. Hanscom, Mass.
13. Fennell, J.F. (1982), Description of P78-2 (SCATHA) satellites and experiments, in The IMS Source Book: Guide to the International Magnetospheric Study Data Analysis, edited by C.T.Russell and D.J.Southwood, 65-81, AGU, Washington D.C.
14. Lai, S. T., and Maurice Tautz (2008), On the anticritical temperature for spacecraft charging, Journal of Geophysical Research, 113, A11211, doi:10.1029/2008JA013161
15. Whipple, E. C. (1981), Potentials of surfaces in space, Reports on Progress in Physics, 44, 1197-1250.
16. Darlington, E. H. and Cosslett, V. E. (1972), Backscattering of 0.5-10 keV Electrons From Solid Targets, J. Phys.D., App. Phys., 5, 1961-1981.